

# PLANAR PARALLEL 3-RPR MANIPULATOR

**Robert L. Williams II**

**Atul R. Joshi**

Ohio University  
Athens, OH 45701

**Proceedings of the Sixth Conference on Applied Mechanisms and Robotics**  
Cincinnati OH, December 12-15, 1999

Contact author information:

**Robert L. Williams II**

Assistant Professor

Department of Mechanical Engineering

257 Stocker Center

Ohio University

Athens, OH 45701-2979

phone: (740) 593 - 1096

fax: (740) 593 - 0476

email: bobw@bobcat.ent.ohiou.edu

URL: <http://www.ent.ohiou.edu/~bobw>

# Planar Parallel 3-*RPR* Manipulator

Robert L. Williams II and Atul R. Joshi

Department of Mechanical Engineering

Ohio University

bobw@bobcat.ent.ohiou.edu

## ABSTRACT

This paper describes the design, construction, and control of a planar three degree-of-freedom (*dof*) in-parallel-actuated manipulator at Ohio University. The actuators are three pneumatic cylinders. Using real-time closed-loop feedback control for each actuator length independently, we develop inverse pose and resolved-rate control for this manipulator. The objective of this work is to implement in hardware a 3-*RPR* manipulator design and to evaluate parallel manipulator control using pneumatics. The manipulator has been built and controlled in real-time.

## 1. INTRODUCTION

Parallel manipulators are robots that consist of separate serial chains that connect the fixed link to the end-effector link. The following are potential advantages over serial robots: better stiffness and accuracy, lighter weight, greater load bearing, higher velocities and accelerations, and less powerful actuators. A major drawback of the parallel robot is reduced workspace.

Parallel robotic devices were proposed by MacCallion and Pham (1979). Some configurations have been built and controlled (e.g. Sumpter and Soni, 1985). Numerous works analyze kinematics, dynamics, workspace and control of parallel manipulators (see Williams, 1988 and references therein). Hunt (1983) conducted preliminary studies of various parallel robot configurations. Cox and Tesar (1981) compared the relative merits of serial and parallel robots.

Aradyfio and Qiao (1985) examined the inverse kinematics solutions for three different 3-*dof* planar parallel robots. Williams and Reinholtz (1988a and

1988b) study dynamics and workspace for a number of parallel manipulators. Shirkhodaie and Soni (1987), Gosselin and Angeles (1988), and Pennock and Kassner (1990) each present a kinematic study of one planar parallel robot. Gosselin et al. (1996) present the position, workspace, and velocity kinematics of one planar parallel robot.

Recently, more general approaches have been presented. Daniali et al. (1995) present an in-depth study of actuation schemes, velocity relationships, and singular conditions for general planar parallel robots. Gosselin (1996) presents general parallel computation algorithms for kinematics and dynamics of planar and spatial parallel robots. Merlet (1996) solved the forward pose kinematics problem for a broad class of planar parallel robots. Williams and Shelley (1997) solved the inverse pose and velocity kinematics problem for this same class.

The current paper presents a 3-*RPR* planar parallel robot which has been designed, built, and controlled at Ohio University. The paper first presents the manipulator description including kinematics, followed by a design and construction discussion and then the control architecture.

## 2. 3-*RPR* DESCRIPTION

The manipulator considered in this paper is symmetric and composed of three identical legs connecting the fixed base to the end-effector triangle as shown in Fig. 1. Each leg is of *RPR* design, with two passive revolute joints and an active prismatic joint in-between. Each prismatic joint is an actively-controlled pneumatic cylinder.

## 2.1 Kinematics

The 3-RPR kinematic diagram is given in Fig. 2. The three grounded passive revolute joints are located on the base triangle at  $\underline{A}_i$  and the three moving passive revolute joints are located on the moving triangle at  $\underline{C}_i$ , where  $i=1,2,3$ . The active prismatic joint variables are the total lengths  $L_i$ , giving the length between passive revolute joints. The moving frame  $\{H\}$  is at the triangle centroid and the base frame  $\{B\}$  is shown in Fig. 2. The Cartesian variables are the triangle link pose  $X = \{x \ y \ \phi\}^T$ . The Grubler mobility equation predicts this device has three degrees-of-freedom, by counting eight rigid links connected by nine one-dof joints.  $\theta_i$  are passive intermediate joint angles which are not required for hardware control, but which may be calculated for computer simulation and/or velocity and dynamics calculations.

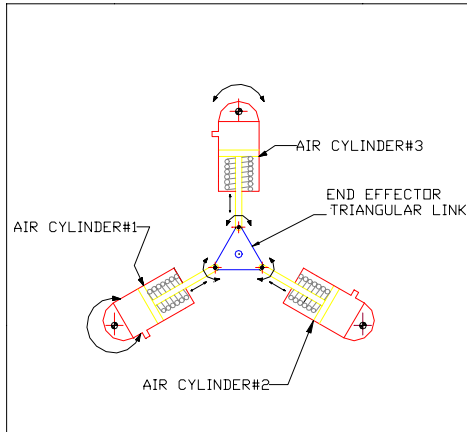


Figure 1. 3-RPR Manipulator

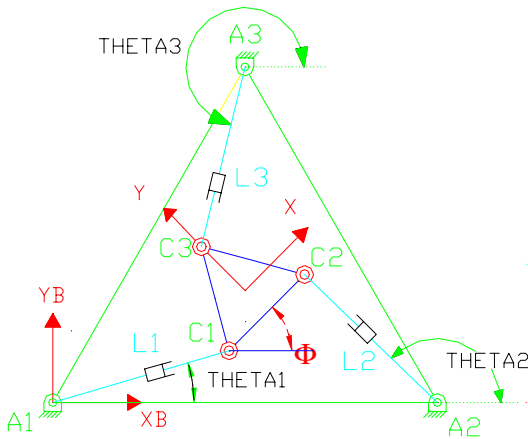


Figure 2. 3-RPR Kinematic Diagram

**2.1.1 Inverse Pose Kinematics.** The inverse pose problem is stated: Given the desired Cartesian pose  $X = \{x \ y \ \phi\}^T$ , calculate the required prismatic joint lengths  $L = \{L_1 \ L_2 \ L_3\}^T$ . There is a duality with serial manipulators: generally the inverse kinematics is straight-forward, while the forward kinematics problem is difficult, which is opposite the case for serial manipulators. For the 3-RPR, since we are given the pose  $X$ , we can easily calculate moving revolute locations  $\underline{C}_i$  and then the inverse pose solution is simply finding the vector lengths  $L_i$  between  $\underline{C}_i$  and  $\underline{A}_i$ ,  $i=1,2,3$ . For each RPR leg, the following vector loop closure equation may be written:

$${}^B \underline{C}_i = {}^B \underline{P}_H + {}^B {}_H R^H \underline{C}_i = {}^B \underline{A}_i + L_i e^{i\theta_i} \quad i=1,2,3 \quad (1)$$

where:  ${}^B \underline{P}_H = \begin{Bmatrix} x \\ y \end{Bmatrix}$  and  ${}^B {}_H R = \begin{bmatrix} c\phi & -s\phi \\ s\phi & c\phi \end{bmatrix}$

$$c\phi = \cos \phi \quad s\phi = \sin \phi$$

We calculate  ${}^B \underline{C}_i = {}^B \underline{P}_H + {}^B {}_H R^H \underline{C}_i$  from the given  $X$  and known robot geometry and then the solutions are found using the Euclidean norm in (2):

$$L_i = \left\| {}^B \underline{C}_i - {}^B \underline{A}_i \right\| \quad i=1,2,3 \quad (2)$$

The intermediate passive joint angles  $\theta_i$  are:

$$\theta_i = a \tan 2 \left( {}^B C_{iy} - {}^B A_{iy}, {}^B C_{ix} - {}^B A_{ix} \right) \quad i=1,2,3 \quad (3)$$

**2.1.2 Forward Pose Kinematics.** The forward pose problem is stated: Given the current prismatic joint lengths  $L = \{L_1 \ L_2 \ L_3\}^T$ , calculate the Cartesian pose  $X = \{x \ y \ \phi\}^T$ . This problem requires the solution of coupled nonlinear equations. The same vector loop closure equations (1) apply, rewritten in (4),  $i=1,2,3$ :

$$\begin{Bmatrix} L_i c\theta_i \\ L_i s\theta_i \end{Bmatrix} = \begin{Bmatrix} x \\ y \end{Bmatrix} + \begin{bmatrix} c\phi & -s\phi \\ s\phi & c\phi \end{bmatrix} \begin{Bmatrix} {}^H C_{ix} \\ {}^H C_{iy} \end{Bmatrix} - \begin{Bmatrix} {}^B A_{ix} \\ {}^B A_{iy} \end{Bmatrix} \quad (4)$$

Equation (4) includes all unknowns  $X = \{x \ y \ \phi\}^T$  and one passive unknown  $\theta_i$ . One approach to solve this problem is to apply the numerical Newton-Raphson method. First, since  $\theta_i$  is not required, we can square and add the  $x$  and  $y$  component equations in (4) to eliminate  $\theta_i$ . The result is three equations coupled and nonlinear in the unknowns  $X$ . Solution details are not given here.  $\theta_i$  can be found after  $X$  is known using (3).

This forward pose problem is equivalent to finding the assembly configurations of a four-bar linkage with input/output links  $L_1, L_2$  and an  $RR$  constraining dyad of length  $L_3$ . By itself the four-bar linkage has infinite assembly configurations because it has one-*dof*.  $RR$  dyad  $\underline{A}_3\underline{C}_3$  constrains the mechanism to a statically-determinate structure of 0-*dof*. Point  $\underline{C}_3$  defines a four-bar coupler curve which is a tricircular sextic (sixth-degree algebraic curve) that has a maximum of six intersections with the circle of radius  $L_3$  centered at  $\underline{A}_3$  (Hunt, 1990). This is an alternative analytical solution.

**2.1.3 Velocity Kinematics.** Inverse velocity kinematics is used for resolved-rate control and forward velocity kinematics may be used for simulation. To derive the velocity relationships, the vector loop closure equations are rewritten again:

$${}^B P_H = {}^B A_i + L_i e^{i\theta_i} + l_{Hi} e^{i(\theta_i + \beta_i)} \quad i = 1, 2, 3 \quad (5)$$

where  $l_{Hi}$  is the length from  $\underline{C}_i$  to the origin of  $\{H\}$  and  $\beta_i$  is the variable angle, related to  $\phi$ , from the end of the  $L_i$  direction to the current direction of  $l_{Hi}$ .

The inverse velocity problem is stated: Given the manipulator configuration and the desired Cartesian rates  $\dot{X} = \{\dot{x} \ \dot{y} \ \dot{\phi}\}^T$ , calculate the required prismatic joint rates  $\dot{L} = \{\dot{L}_1 \ \dot{L}_2 \ \dot{L}_3\}^T$ . The velocity kinematics method for all planar parallel manipulators is presented in Williams and Shelley (1997); the method is briefly summarized here and the results are given for the 3-RPR. Taking a time derivative of (5) yields a velocity equation which can be arranged as a 3x3 Jacobian matrix mapping joint rates  $\dot{\rho}_i = \{\dot{\theta}_i \ \dot{L}_i \ \dot{\beta}_i\}^T$  into Cartesian rates  $\dot{X} = \{\dot{x} \ \dot{y} \ \dot{\phi}\}^T$ . Since we only desire the active joint

rates  $\dot{L}_i$ , we invert this Jacobian relationship. Then, the  $\dot{L}_i$  row only is extracted; this is repeated for  $i=1,2,3$ . The overall Jacobian relationship for the 3-RPR results:

$$\begin{Bmatrix} \dot{L}_1 \\ \dot{L}_2 \\ \dot{L}_3 \end{Bmatrix} = \begin{bmatrix} c\theta_1 & s\theta_1 & l_{H1}s\beta_1 \\ c\theta_2 & s\theta_2 & l_{H2}s\beta_2 \\ c\theta_3 & s\theta_3 & l_{H3}s\beta_3 \end{bmatrix} \begin{Bmatrix} \dot{x} \\ \dot{y} \\ \dot{\phi} \end{Bmatrix} \quad (6)$$

Note (6) directly gives the inverse velocity solution which can be abbreviated  $\dot{L} = M\dot{X}$ , where  $M$  is the 3x3 inverse manipulator Jacobian matrix. The forward velocity solution is then  $\dot{X} = M^{-1}\dot{L}$ . Hence we find another serial/parallel robot duality: the 3-RPR inverse velocity problem is not subject to singularities, while the forward velocity problem is.

All kinematics solutions have been implemented in Matlab; the real-control control architecture presented later uses Matlab directly. An example animation snapshot from Matlab is given in Fig. 3.

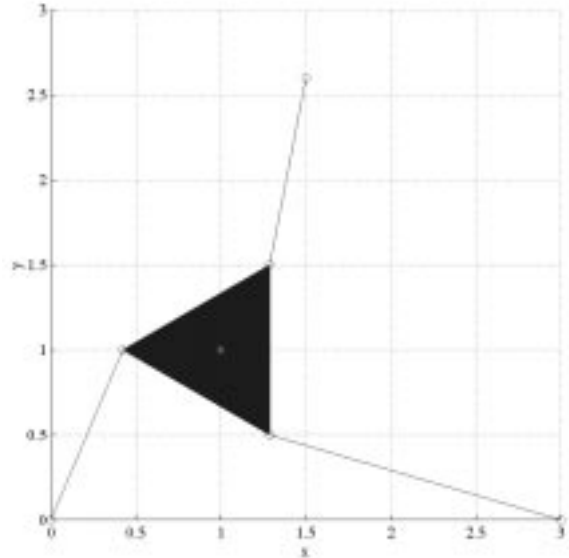


Figure 3. 3-RPR Matlab Snapshot

## 2.2 Workspace

Limited workspace is the principal disadvantage of parallel robots. Therefore, we are using a geometric method (Williams, 1988) to determine the 3-RPR workspace and design the manipulator parameters to maximize the workspace. This effort is not complete, but

the hardware has been built to allow for different ground revolute locations  $A_i$  to evaluate workspace results in the future, constrained by the hand triangle link (which we can also change) and the prismatic joint limits. Figure 4 shows a sample reachable workspace result for the 3-RPR.

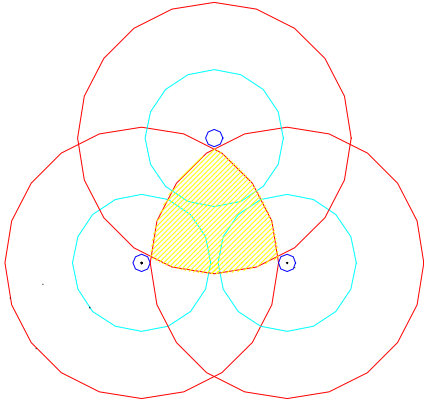


Figure 4. Example 3-RPR Reachable Workspace

### 3. 3-RPR DESIGN AND CONSTRUCTION

This section discusses the design and construction of 3-RPR hardware at Ohio University. The budget for this project was small, so the most important design specification was to make use of existing actuators, sensors, control elements, and I/O boards. Also, since most robotic projects at Ohio University make use of DC servomotors, it was desired to use pneumatic power for a change of pace. This dictated the use of existing pneumatic air cylinders (spring loaded to return to minimum joint length), linear variable displacement transducer (LVDT) length sensors, solenoid valves to regulate air flow to the cylinders, and a PC-based control system using Quanser Multi-Q I/O boards. The three RPR legs are identical, with three independent pneumatic cylinders and LVDTs across each. An oil-less air compressor is the pneumatic power source, providing 120 psi, regulated to a constant 60 psi which is delivered through a three-way hose coupling manifold to each solenoid valve to power the cylinders. Components which were procured included pneumatic plumbing elements, Delrin plastic for the hand triangle, link extensions, and ground fixtures, plus bolts for the passive revolute joints.

The 3-RPR robot hardware is shown in Fig. 5. In Fig. 5 the pneumatic cylinders are on the bottom while the LVDTs are mounted parallel to the cylinders on top. The PC I/O boards, the three solenoid valves, and the electric power supply for the solenoid valves and LVDTs are shown (left-to-right) in Fig. 6. The pneumatic power supply is not pictured.

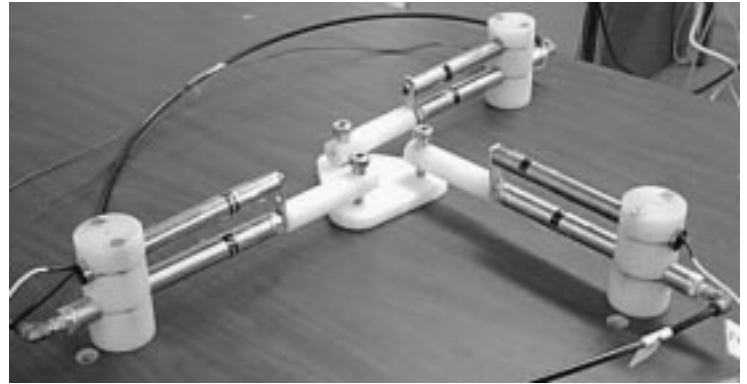


Figure 5. 3-RPR Hardware

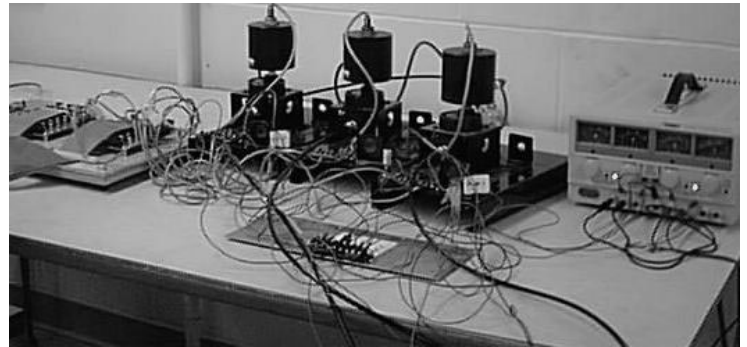


Figure 6. I/O Boards, Solenoid Valves, and Power Supply

The next section presents the 3-RPR control architecture. First, on the following page Fig. 7 presents the overall 3-RPR system diagram which connects mechatronic design and control architecture for the 3-RPR hardware.

Three pneumatic cylinder/LVDT units are connected to the pneumatic power supply as described earlier and also connected to the control PC. Each cylinder receives air pressure by commanding voltage to the solenoid

valve. The resulting length motion is detected by the LVDT sensor which is sent to the PC. There is an external Multi-Q MQ3 I/O board which interfaces to an internal Multi-Q control board. Not shown in Fig. 7 is the electric power supply which supplies  $\pm 15$  volts to the LVDTs and +15 volts to the solenoid valves. The PC reads the output LVDT analog voltage value and commands appropriate voltage values to each solenoid valve. Control details are discussed in the next section.

#### 4. 3-RPR CONTROL

The 3-RPR hardware real-time control architecture is discussed in this section. The 3-RPR can be controlled in joint mode, either open-loop or closed loop with LVDT length feedback. The 3-RPR can also be controlled in Cartesian mode (inverse pose control or resolved-rate control using inverse velocity) which in turn requires closed-loop control of all three pneumatic actuators simultaneously.

The required kinematic solutions (discussed in section 2) for control are implemented in Matlab's Simulink graphical interface. As shown in Fig. 7, Simulink model output commands real-world hardware via the Quanser Wincon software and internal and external Multi-Q boards. In the open-loop case, the Simulink model commands desired voltage values to the solenoid valves which operate the pneumatic cylinders without LVDT feedback. In the closed-loop case (joint control, Cartesian pose control, or Cartesian velocity control), the Simulink model commands voltage values to the solenoid values based on values calculated by the on-line controller for achieving the three desired link lengths. Solenoid voltage commands go out and the LVDT voltage readings come into the PC via the external I/O board and internal board, which interfaces with Simulink via Wincon software. Three analog inputs and three analog outputs on the external boards are used, one for each pneumatic cylinder/LVDT combination.

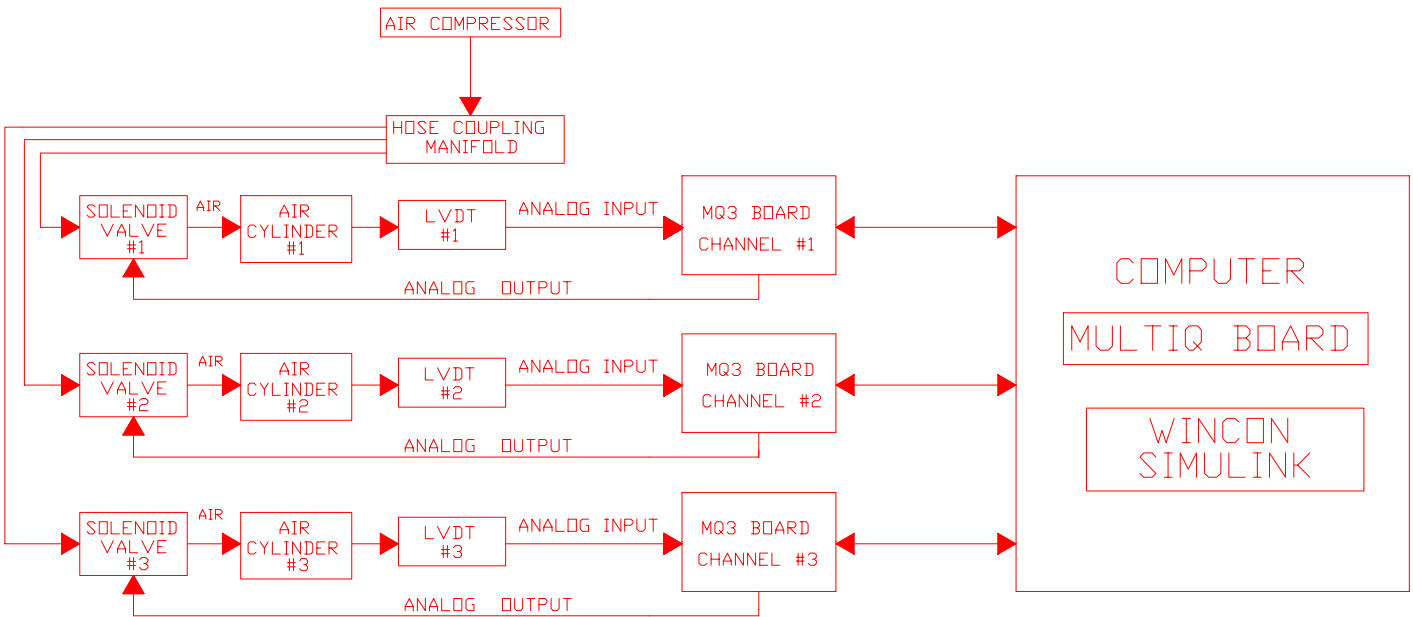


Figure 7. Overall 3-RPR System Diagram

Figure 8 shows the closed-loop feedback control block diagram for achieving the desired commanded pneumatic cylinder lengths. The block diagram is for one cylinder; all three use the same block diagram.

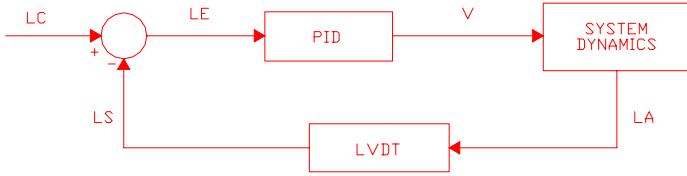


Figure 8. Leg Length Control Block Diagram

In Fig. 8,  $L_C$  is the commanded leg length for prismatic actuator  $i$ .  $L_E$  is the length error.  $V$  is the solenoid voltage to be applied, calculated by the proportional-integral-derivative (PID) control law.  $L_A$  is the actual pneumatic cylinder length resulting from this voltage command (and the ensuing dynamic response of the entire system, i.e. three actuators operating simultaneously).  $L_S$  is the sensed value of this actual length, as read by the LVDT feedback.

In this manner we achieve coordinated Cartesian control of the 3-RPR via linearized independent (but simultaneous) prismatic joint control. We have not derived the system dynamics block for Fig. 8; in fact, the Simulink diagram implementation of Fig. 8 is open at this block (the real-world hardware closes the loop). Rather, the PID gains have been determined experimentally by setting the proportional gain first (starting with low values and working up!) and adding the integral and derivative terms as needed (again, starting with low values). We use the Simulink PID block (with approximate derivative to minimize the problems with numerical differentiation).

In the hardware control implementation, it was found that a PD controller worked well. The D term was essential to maintain stability, which is expected from theory. The I term is supposed to reduce the steady-state error, but was set to zero in the 3-RPR; other I values caused erratic, marginally stable results. Each pneumatic cylinder has a stiff spring which returns the prismatic joint length to the minimum limit when the pressure is released (or at a low value). It was found that this spring stiffness dominated the response. In the near future we are planning to implement a feedforward term in Fig. 8 to neutralize the effect of this spring (depending on the

magnitude of the commanded length  $L_C$ ) so the PID controller can be concerned with fine positioning control.

Figure 9 shows the PC screen during experimental length control of one pneumatic cylinder. The background window is the Simulink model controlling the 3-RPR hardware. The lower small window on the right is the Wincon window. The small window directly above that is the real-time numerical display of the LVDT's measurement of this pneumatic cylinder length. The graph window on the left displays in real-time the time history of this controlled length.

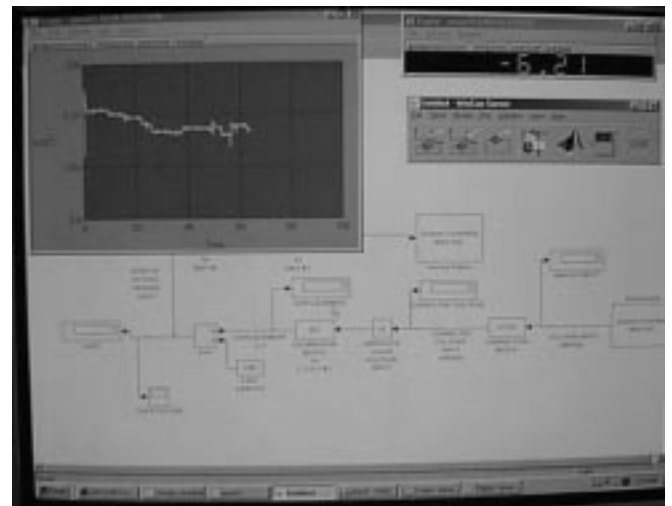


Figure 9. Simulink/Wincon Interface to the 3-RPR

## 5. CONCLUSION

This paper has presented kinematics, hardware construction, and control architecture for the planar parallel 3-RPR manipulator built at Ohio University. This three degree-of-freedom manipulator is actuated by pneumatic cylinder prismatic joints. The revolute joints are all passive. In a limited workspace the robot can reach general planar poses (translation and rotation). Applications for this type of robot include manufacturing and assembly where high speed and accuracy are required in a relatively small workspace. Other applications are planar motion simulators and haptic interfaces.

The 3-RPR hardware is controlled in real-time via a PC with a Matlab Simulink model reading LVDT

feedback and commanding solenoid valves via the Quanser Multi-Q boards and Wincon software. The control architecture controls the three pneumatic cylinder lengths independently but simultaneously in this environment. Open-loop leg control is possible, as well as leg length control and Cartesian pose and velocity control using LVDT feedback for closed-loop pneumatic cylinder control. This type of control was found to be effective in experiments. More experiments will be conducted to assess the strengths and weaknesses of the as-built system. Future work includes evaluation of this type of parallel hardware compared with serial robots. Also, comparing pneumatic control with DC servomotor actuation can now be performed.

## REFERENCES

- D.D. Aradyfio and D. Qiao, 1985, "Kinematic Simulation of Novel Robotic Mechanisms Having Closed Chains", *ASME Paper 85-DET-81*.
- D.J. Cox and D. Tesar, 1981, "The Dynamic Modeling and Command Signal Formulation for Parallel Multi-Parameter Robotic Devices", DOE Report.
- H.R.M. Daniali, P.J.Z. Zsomer-Murray, and J. Angeles, 1995, "Singularity Analysis of Planar Parallel Manipulators", **Mechanism and Machine Theory**, Vol. 30, No. 5, pp. 665-678.
- C.M. Gosselin, 1996, "Parallel Computation Algorithms for the Kinematics and Dynamics of Planar and Spatial Parallel Manipulators", **Journal of Dynamic Systems, Measurement, and Control**, 118 (1): 22-28.
- C.M. Gosselin, S. Lemieux, and J.P. Merlet, 1996, "A New Architecture of Planar Three-Degree-of-Freedom Parallel Manipulator", *IEEE International Conference on Robotics and Automation*, Minneapolis, MN, 4: 3738-3743.
- C.M. Gosselin and J. Angeles, 1988, "The Optimum Kinematic Design of a Planar Three-Degree-of-Freedom Parallel Manipulator", **ASME Journal of Mechanisms, Trans., and Automation in Design**, 110(1): 35-41.
- K.H. Hunt, 1990, Kinematic Geometry of Mechanisms, Clarendon Press, Oxford.
- K.H. Hunt, 1983, "Structural Kinematics of In-Parallel-Actuated Robot Arms", **Journal of Mech., Trans., and Automation in Design**, 105(4).
- H. MacCallion and D.T. Pham, 1979, "The Analysis of a Six-Degree-of-Freedom Workstation for Mechanized Assembly", *5<sup>th</sup> World Congress on TMM*, Montreal.
- J.P. Merlet, 1996, "Direct Kinematics of Planar Parallel Manipulators", *IEEE International Conference on Robotics and Automation*, 4: 3744-3749.
- G.R. Pennock and D.J. Kassner, 1990, "Kinematic Analysis of a Planar Eight-Bar Linkage: Application to a Platform-type Robot", *ASME Mechanisms Conference*, DE-25: 37-43.
- A.H. Shirkhodaie and A.H. Soni, 1987, "Forward and Inverse Synthesis for a Robot with Three Degrees of Freedom", *Summer Computer Simulation Conference*, Montreal, 851-856.
- B. Sumpter and A.H. Soni, 1985, "Simulation Algorithm of Oklahoma Crawdad Robot", *9<sup>th</sup> Applied Mechanisms Conference*, Kansas City, VI.1-VI.3.
- R.L. Williams II, 1988, "Planar Robotic Mechanisms: Analysis and Configuration Comparison", **Ph.D. Dissertation**, VPI&SU, Blacksburg, VA.
- R.L. Williams II and C.F. Reinholtz, 1988a, "Forward Dynamic Analysis and Power Requirement Comparison of Parallel Robotic Mechanisms", *20<sup>th</sup> Biennial ASME Mechanisms Conference*, Kissimmee FL, DE Vol. 15-3, pp. 71-78.
- R.L. Williams II and C.F. Reinholtz, 1988b, "Closed-Form Workspace Determination and Optimization for Parallel Robotic Mechanisms", *20<sup>th</sup> Biennial ASME Mechanisms Conference*, Kissimmee FL, DE 15-3: 341-351.
- R.L. Williams II and B.H. Shelley B.H., 1997, "Inverse Kinematics for Planar Parallel Manipulators", *23<sup>rd</sup> ASME Design Automation Conference, DETC97/DAC-3851*, Sacramento, CA, September 14-17.